Poly(ethylene terephthalate) surface dynamics in air and water studied by tensiometry and molecular modelling

C. Vergelati, A. Perwuelz* and L. Vovelle
Rhône-Poulenc Recherches, Centre de Recherches des Carrières, BP 62, 69192 Saint-Fons Cedex, France

and M. A. Romero and Y. Holl‡
Institut Charles Sadron (EAHP-CRM), 4 rue Boussingault, 67000 Strasbourg, France
(Received 11 August 1992; revised 19 April 1993)

The wetting characteristics of an amorphous poly(ethylene terephthalate) (PET) film by water were studied by the Wilhelmy plate technique in the dynamic and static modes. At room temperature, a dynamic hysteresis of 40° ($\theta_A = 80°$, $\theta_R = 40°$) was found. It was interpreted in terms of water adsorption–desorption phenomena. The air–water and water–air equilibration processes of the PET surface were studied. The static mode was most useful for this purpose. It showed that it takes about 10 days to reach equilibrium at 20°C and that equilibration with water is only partially reversible. Surface restructuration was described by molecular modelling. The validity of this description was confirmed by a good quantitative agreement between experimental and calculated data. An increase of the temperature accelerates molecular rearrangements especially around the glass transition temperature of the polymer.

(Keywords: poly(ethylene terephthalate); surface orientation; contact angle hysteresis)

INTRODUCTION

Depending on the environment, the macromolecules at the surface of a solid polymer may change their conformations in order to minimize the interfacial energy. In contact with water, a macromolecule having both hydrophilic and hydrophobic moieties in its structure may tend to restructure to expose its polar parts to water and bury its apolar parts. The opposite process will occur in air. According to Lavielle's[1] bibliographic survey, Langmuir[2] first proposed the idea of surface restructuration in the case of stearic acid salt layers coating a substrate. The concept was extended to polymeric chains (acrylic hydrogels) by Holly and Rejofo[3]. Subsequently, several authors have shown the occurrence of conformational alterations at the surface of various types of polymeric materials: block copolymers like segmented poly(ether urethane)s and poly(ether urethane urea)s[4], hydrophobic polymers grafted with hydrophilic molecules (acrylic acid-grafted polyethylene)[5], plasma-treated polymers[6] and even hydrophobic polymers like polytetrafluoroethylene[7]. Techniques like dynamic contact angle measurements, inverse gas chromatography[8], classical methods to measure polymer transitions and relaxations in highly filled polymers, X-ray photoelectron spectroscopy and nuclear magnetic resonance were used in these studies. The restructuration strongly influences wettability, adhesion and biological properties of polymeric materials. Andrade[9–12] contributed much to the popularity of this concept of surface dynamics of polymers. It is currently commonly taken as a matter of fact, for example in the field of polymer colloids[13], although some prominent authors still do not yet discuss the subject properly[14].

Some attempts have been made to go into more details of the process. Lavielle *et al.*[15] suggested the use of thermodynamics of irreversible processes. Another approach has been to apply simple models based on electrostatic theory[16,17], in order to explain wetting hysteresis in terms of chain reorientation. An important point to consider is the time course of the phenomenon. The kinetics of restructuration of surfaces depends on the mobility of the surface chains. Consequently, it is a temperature-dependent process. One may expect the mobility of chains to be higher at the surface than in the bulk, although there is no clear experimental evidence of this. However, an interesting work by Pennings and Bosman[18] showed that activation energies of relaxations at the surface are very closely related to activation energies of bulk relaxations, which seems to indicate that molecular mobility at the surface is not really higher than in the bulk. This point needs to be further investigated.

Another possibility, in order to understand the phenomenon of surface restructuration, is to use conformational analysis by molecular modelling. The aim of conformational calculations is to describe and predict the possible conformations of molecules. The principle is the following. One starts with the monomer unit separated into flexible and rigid parts. The different conformations of the monomer unit are due to the

---

* Present address: ENSAIT/GENITEX, 59070 Roubaix Cedex 1, France

‡ To whom correspondence should be addressed

0032-3861/94/020262-09

motions of the flexible parts. Molecular mechanics[19-22] is used to determine each conformation with the lowest energy. The conformations of a macromolecular chain then result from a statistical succession of monomer units in low-energy conformations according to a Boltzmann distribution. The probability of occurrence of a monomer conformation of energy E_c is proportional to $\exp(-E_c/RT)$. The key authors in the field of conformational chain statistics are Volkenstein[23], who introduced the matricial formalism, and Flory[24]. The RIS (rotational isomeric state) model, developed by Flory[25], is most widely used.

Once the conformations of a macromolecule have been described in the absence of any external interactions, the next step is to consider the influence of a surrounding medium, like a solvent. When a polymeric chain is put into a solvent and interacts with the solvent molecules, the resulting energy can be written as follows:

$$G_{tot} = G_{conf} + G_{cav} + G_{elect} + G_{disp}$$

with G_{conf} being the conformational energy of the 'free' molecule and $G_{cav} + G_{elect} + G_{disp}$ the solvation energy. The solvent is considered as a dielectric continuum. The actual dissolving process is twofold: (i) Creation of a cavity where the molecule can be accommodated; this requires work to overcome the cohesion energy of the solvent (cavitation energy $= G_{cav}$). (ii) Interaction of the molecule with the surrounding medium (energy of interaction $= G_{elect} + G_{disp}$, with G_{elect} resulting from electrostatic contributions and G_{disp} from dispersive interactions). The cavitation step (G_{cav}) has been modelled by Pierotti[26], and, in a more sophisticated way, by Tvaroska and Kozar[27].

We were interested in the study of molecular rearrangements at the surface of poly(ethylene terephthalate) (PET) in contact with air and then water. This polymer has many uses as a film for magnetic or packaging applications. In order to improve the surface properties of the film, it can be coated by an aqueous latex, which leaves a thin polymeric layer at its surface after water evaporation. The wetting characteristics of the PET film by an aqueous phase and the adsorption of the latex constituents at the surface of PET are of major importance. Wetting and adsorption are strongly dependent on the actual surface structure of PET in air and water.

We investigated the surface structure of PET by dynamic and static contact angle measurements in water using the Wilhelmy plate technique. We observed contact angle hysteresis, which we interpreted in terms of water adsorption and molecular rearrangements. Finally, we tried to describe these rearrangements by molecular modelling.

EXPERIMENTAL

Poly(ethylene terephthalate) (PET) film

The PET film (supplied by Rhône-Poulenc) was amorphous, 250 μm thick, with a roughness around 10 nm estimated from SEM pictures. The sample size was about 14×14 mm^2. It was rigid enough to be used as the plate without difficulties in the Wilhelmy plate procedure (see below). The films were decontaminated using butanol, rinsing them in doubly distilled water and drying them in a vacuum desiccator at 30°C for 14 h. Electron spectroscopy for chemical analysis (e.s.c.a.) (VG Escalab Mk II) revealed no elements other than carbon and oxygen in the surface layer even after a long period of time in water.

The Wilhelmy plate technique

The principle of this technique is explained in detail in ref. 28. It consists of dipping a solid sample with a simple shape (plate, rod, tube, ...) into a liquid while recording the force exerted on it. The force is given by:

$$F = mg + \gamma_1 P \cos\theta - F_b$$

where mg = weight of the sample, γ_1 = surface tension of the liquid, P = perimeter of the sample, θ = solid–liquid contact angle and F_b = buoyancy force.

When a totally wetted plate with a well defined perimeter is used, the contact angle is zero and the surface tension of the liquid can be easily calculated. When a liquid with known γ_1 is used, the solid–liquid contact angle can be determined. This technique is highly accurate and precise. It was proposed by Wilhelmy[29] in the last century. It was first used for liquid surface tension measurements[30]. Johnson and Dettre[31] developed the method for the determination of liquid–solid contact angles. The contact angle when the sample is immersed in the liquid (advancing contact angle, θ_A) is often different from the one when the sample is withdrawn (receding contact angle, θ_R). The difference, $\Delta\theta = \theta_A - \theta_R$, is called the contact angle hysteresis. This hysteresis can be due to several factors: surface roughness or heterogeneity, solid deformation, swelling and penetration of the liquid in the surface layer, surface mobility and restructuration, as well as surface entropy. The magnitude of the hysteresis is then a valuable source of information on the surface layer of the solid in contact with the liquid, but its interpretation is not always straightforward.

For dynamic experiments, we used a Lauda TE1 tensiometer equipped with a measuring chamber, which was temperature-controlled within ±0.1°C. The speed range was 3.25 to 25 mm min^{-1}. In this range, the effect of the immersion–emersion speed was very weak. We shall only present results obtained at the lowest speed. The test liquid was always doubly distilled water. The surface tension of the water was measured after each cycle using a platinum ring in order to check for a leachable contaminant coming out from the film. For each film, immersion–emersion cycles were repeated until reaching an equilibrium state where two consecutive cycles were superposed. The reproducibility of the contact angle measurements was checked by repeating all experiments three times. Within an experimental error of 1–3°, the reproducibility was good. The error depends on the absolute value of the contact angle: the lower the contact angle, the higher the error. Apart from one case (see below), all experiments were performed at 25°C.

We studied the effect of a long contact time (150 h) of the PET with water using the following procedure. The film was dipped in doubly distilled water at room temperature, taken out at various times to measure the contact angle with water by the Wilhelmy technique and then put back into fresh doubly distilled water.

Then a new film was left in water for 70 h and studied after various contact times with air (in a desiccator).

Finally, experiments were performed at different temperatures of the test water: from room temperature to 70°C. Higher temperatures could not be used because of condensation of water onto the PET film.

The Wilhelmy plate technique was also used in the static mode. The PET film was hung onto a balance by a thin thread and dipped into doubly distilled water. About half of the height of the film was in contact with water. This water was contained in a glass bottle, closed except for a small hole, about one millimetre in diameter, to allow the passage of the thread. The level of the water was visually controlled on a scale drawn on the bottle. It remained constant during all experiments. These were performed in a room maintained at a constant temperature of 20°C. The sample was dipped at time zero and left immobile while continuously recording the contact angle as a function of time until equilibrium was reached. It was then withdrawn by 5 mm and the contact angle, corresponding this time to a receding angle, was again recorded as a function of time until equilibrium. Corrections were made to the mass to account for buoyancy effects. The equilibrium swelling of the PET sample by water at 20°C was 1.3 wt%. No detectable size variations of the sample due to swelling occurred.

Conformational calculations

X-ray diffraction data from ethylene glycol dibenzoate[32] were used to provide geometrical parameters (bond lengths and angles) for the PET monomer. As shown by Perez and Brisse[32,33], benzoate groups adopt a planar configuration with very low (less than 4°) angular fluctuations between the aromatic cycle and the carbonyl plane. This group was then considered as rigid in the monomeric unit. The flexible part is the ethylene glycol moiety. All conformations of the monomer unit are generated by torsions along the O–C bond (angle ϕ, see *Scheme 1*) and the C–C bond (angle ψ). These two angles are enough to describe all possible conformations. The interaction energy between non-bonded atoms, the electrostatic energy and the torsional energy (O–C–C sequence) were taken into account for the calculation of the total potential energy. Van der Waals energy (non-bonded interactions) were calculated using Lennard-Jones (6–12) type potential functions with the parameters proposed by Scott and Scheraga[34] for carbon, oxygen and hydrogen. Electrostatic interactions were calculated by ascribing partial charges to all atoms of the molecule and using a Coulomb potential[35] with common parameters for the different bonds[36]. The effective dielectric constant was given a value of 2.0[37]. Potential barriers of order 3 and height 2.8 kcal mol^{-1}, and the same symmetry but height 1.0 kcal mol^{-1}, were assigned to the torsions along the C–C (angle ϕ) and O–C (angle ψ) bonds, respectively[38]. Energies were calculated for each pair of values of ϕ and ψ, every 10° between 0 and 360°. Isoenergetic lines were drawn for 1, 2 and 3 kcal mol^{-1} above the absolute minimum. The representations of the low-energy conformations were drawn with the help of the molecular modelling software Insight II (Biosym. Tec. Inc., San Diego, USA).

Solvation energies (G_{solv}) were calculated using the Solvol software ('Solvol: A Program for Calculating the Energies of Solvation' by I. Tvaroska, Slovak Academy of Science, Bratislava, Czechoslovakia, 1982).

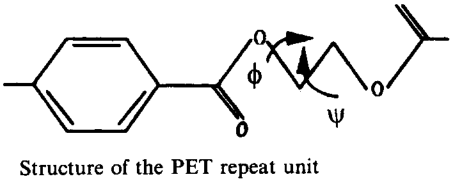

Scheme 1 Structure of the PET repeat unit

These calculations have been performed with water and also, for comparison, with a non-polar solvent, namely diiodomethane (CH_2I_2). For the liquids, the physicochemical parameters necessary for the calculations were collected from the literature[39].

RESULTS

Dynamic tensiometry

Figure 1 shows five successive immersion–emersion cycles of PET in water at 25°C with a speed of 3.25 mm min^{-1}. The advancing contact angle starts at 80° and slightly decreases from one cycle to another until it stabilizes at 75°. This apparent equilibrium value is reached after four cycles. The receding contact angle is almost constant at 40°. The angle very quickly (less than 10 s) changes from its advancing to receding value and vice versa.

Figure 2 presents the advancing and receding angles of water on PET as a function of the contact time of the PET with water. Angles θ_A and θ_R decrease from 80° to 72° and from 40° to 25°, respectively, with increasing contact time in water and apparently stabilize after around 70 h. θ_R decreases more than θ_A, thus the hysteresis value $\Delta\theta$ increases.

The equilibration process of a new sample previously left in water for 70 h was then followed as a function of time in air (*Figure 3*). θ_A and θ_B increase again and $\Delta\theta$ decreases, but the angles seem to stabilize at values lower than the 'air equilibrium values': 75° instead of 80° for θ_A and 35° instead of 40° for θ_R.

The effect of the temperature of the test liquid has also been studied between 25 and 70°C (*Figure 4*). The angles decrease almost linearly when the temperature is raised. For θ_R, one can observe a slope change at the end of the curve.

Static tensiometry

The results of the static tensiometry experiments are shown in *Figure 5*. The time unit of such an experiment

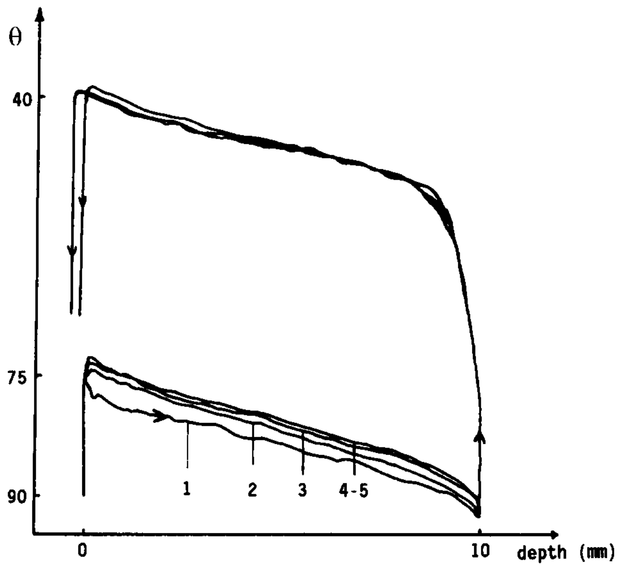

Figure 1 Force exerted on a PET plate *versus* immersion depth in water (five successive cycles). Temperature 25°C. Speed 3.25 mm min^{-1}. The y axis directly shows contact angles calculated from the forces through $\cos\theta = F/\gamma_1 P$

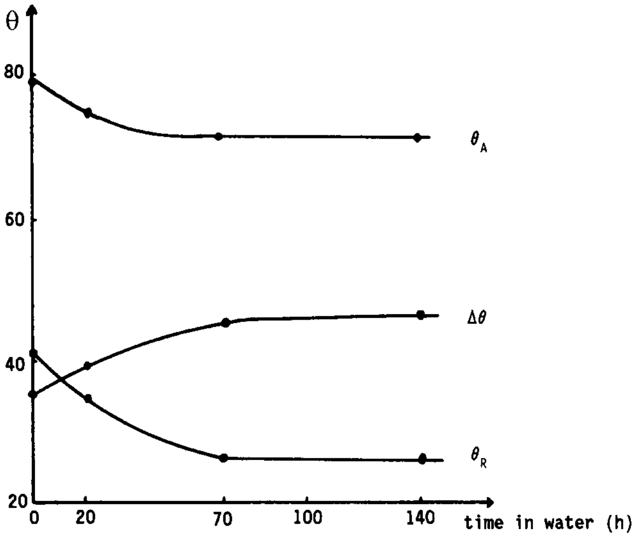

Figure 2 Advancing (θ_A) and receding (θ_R) contact angles of water on PET measured by the Wilhelmy plate technique as a function of time in water. $\Delta\theta = \theta_A - \theta_R$. Temperature 25°C. Speed 3.25 mm min^{-1}

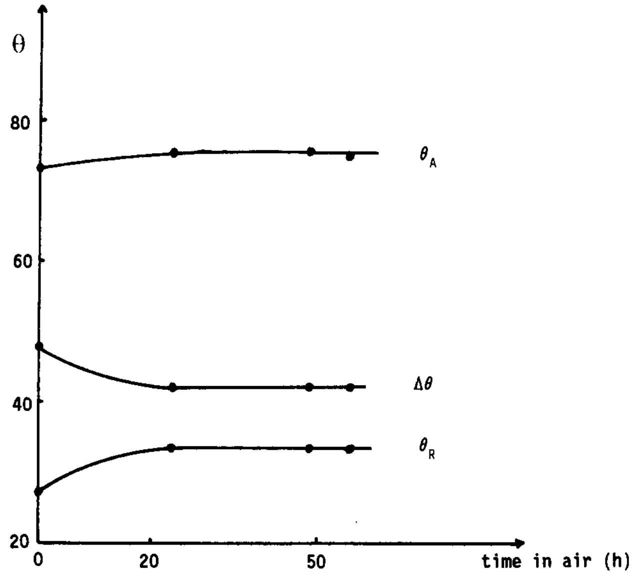

Figure 3 Advancing (θ_A) and receding (θ_R) contact angles of water on PET measured by the Wilhelmy plate technique as a function of time in air of a sample previously left in water for 70 h. $\Delta\theta = \theta_A - \theta_R$. Temperature 25°C. Speed 3.25 mm min^{-1}

is the day. For both advancing and receding angles, equilibrium is reached in 9 to 10 days. The initial value of the advancing angle is 81°. At equilibrium it drops to 70°. The initial and equilibrium receding angles are 53° and 65°, respectively. Consequently, the residual hysteresis is 5°. The decrease of the advancing angle or the increase of the receding angle are not continuous. A kind of pseudo-plateau is reached in about 15 min but then the angles evolve again until the true equilibrium is attained.

Molecular modelling

Figure 6 represents the conformational topology of the repeat unit of PET in the absence of any external influence. There are nine potential wells, at very close energies. The energies are reported in *Table 1*. The probability of occurrence of each conformer in the macromolecular chain was calculated at 298 K (*Table 1*). Owing to the symmetry of the system, there are only five different conformers, represented in *Figure 7*.

The energies of interaction (G_{solv}) of PET with water and CH_2I_2 are shown in *Table 2*. They are referred to the energy of the absolute minimum, which is arbitrarily

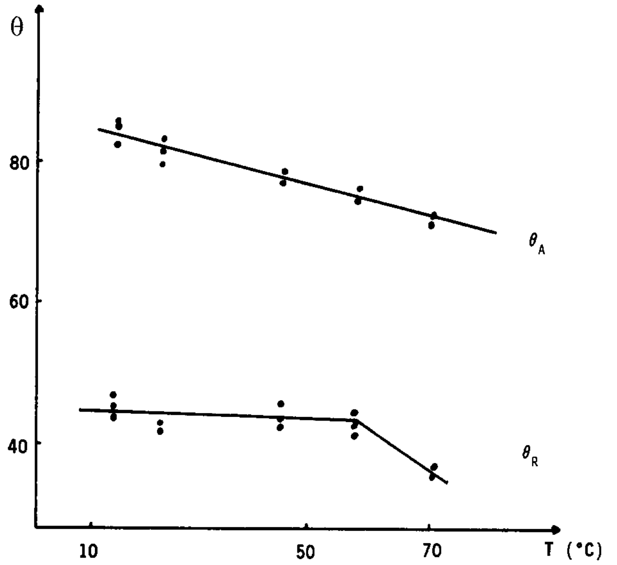

Figure 4 Advancing (θ_A) and receding (θ_R) contact angles of water on PET measured by the Wilhelmy plate technique as a function of the temperature of the test liquid. Speed 3.25 mm min^{-1}

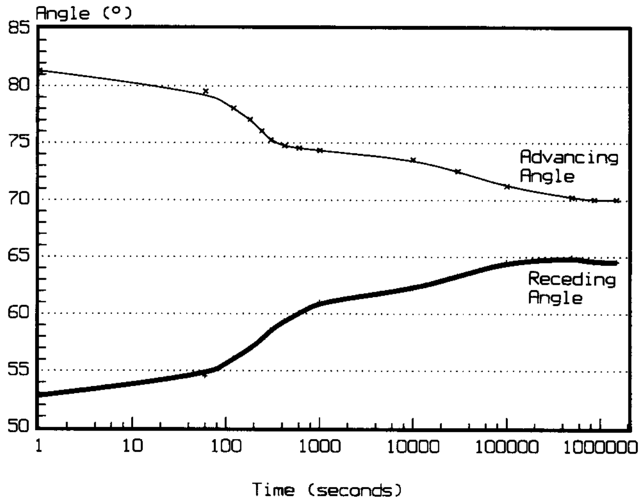

Figure 5 Advancing and receding contact angles of water on PET *versus* time in a static tensiometry experiment

Table 1 Low-energy conformers of the PET repeat unit, associated physical state and conformer distribution in the RIS approximation

Conformer	ϕ, ψ (deg)	Relative energy (kcal mol^{-1})	Associated state	Distribution (%)	
				Org.	Coil
M1	180, 180	0.20	Organized	12.2	
M2	180, 60	0.00	Coil		17.1
M2′	180, −60	0.00	Coil		17.1
M3	−90, 60	0.31	Coil		10.1
M3′	90, −60	0.31	Coil		10.1
M4	80, 60	0.32	Coil		9.9
M4′	−80, −60	0.32	Coil		9.9
M5	80, 180	0.54	Organized	6.8	
M5′	−80, 180	0.54	Organized	6.8	
				25.8	74.2

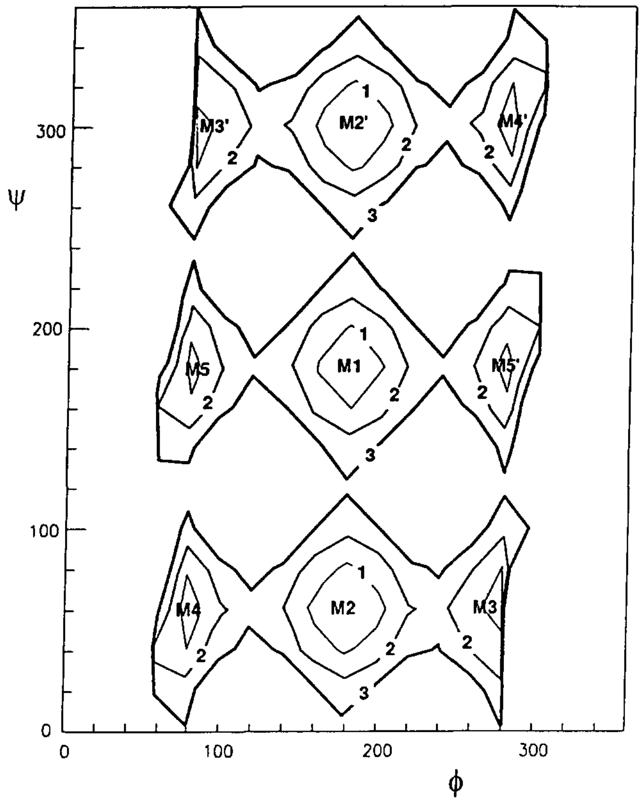

Figure 6 Conformational topology of the PET repeat unit. Isoenergetic lines at 1, 2 and 3 kcal mol^{-1} above the absolute minimum (M2, M2')

Table 2 Solvent effect on the low-energy conformers of the PET repeat unit. G_{solv} and G_{tot} are both referred to their absolute minima (unit:kcal mol^{-1})

	Free state	Water	CH_2I_2
M1 G_{solv}		0.000	0.000
G_{tot}	0.200	0.000	0.090
M2 G_{solv}		1.229	0.110
(M2') G_{tot}	0.000	1.029	0.000
M3 G_{solv}		1.019	0.090
(M3') G_{tot}	0.310	1.129	0.290
M4 G_{solv}		3.097	0.230
(M4') G_{tot}	0.320	3.217	0.440
M5 G_{solv}		0.168	0.010
(M5') G_{tot}	0.540	0.508	0.440

Table 3 Boltzmann distributions of low-energy conformers in the free state, in water and in CH_2I_2, at 298 K

	Free state	Water	CH_2I_2
M1 (%)	12.2	40.0	14.4
M2 (%)	17.1	7.0	16.7
M2' (%)	17.1	7.0	16.7
M3 (%)	10.1	5.9	10.3
M3' (%)	10.1	5.9	10.3
M4 (%)	9.9	0.2	7.9
M4' (%)	9.9	0.2	7.9
M5 (%)	6.8	16.9	7.9
M5' (%)	6.8	16.9	7.9
Organized/coil ratio	25.8/74.2	73.8/26.2	30.2/69.8

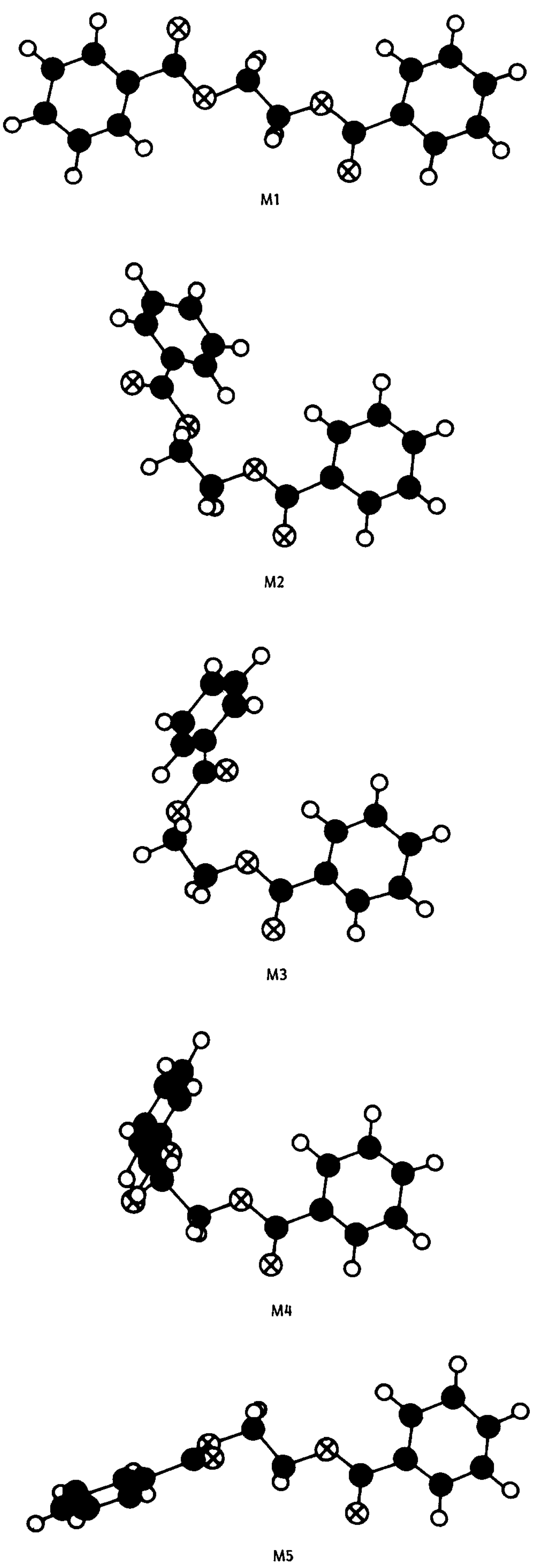

Figure 7 Representation of the five different low-energy conformers of the PET repeat unit: C (●), H (○), O (⊗)

taken as zero. G_{tot} values also figure in *Table 2*, again referred to the absolute minimum of the total energy. Boltzmann distributions of low-energy conformations of the PET repeat unit in the free state, in water and in diiodomethane are shown in *Table 3*.

DISCUSSION

The first point to discuss is the origin of the hysteresis in a standard dynamic tensiometric experiment of PET in water as shown in *Figure 1*. The advancing and receding contact angles differ by 35 to 40°. As a matter of fact, the absence of hysteresis is rather rare in a Wilhelmy experiment. Such a case is presented in ref. 28: for a highly clean mica surface, prehydrated in water, the advancing and receding slopes and angles in water are identical. However, according to Andrade[28], 'contact angle hysteresis is the rule rather than the exception'. A classical example of hysteresis for a polymeric surface is the case of polybutadiene in water where $\Delta\theta$ is around 30° for a freshly prepared sample[40] (contact angles then change due to surface oxidation).

There are several possible causes of hysteresis. The most commonly cited ones are roughness and surface heterogeneity. Johnson and Dettre[41] have shown that hysteresis increases with increasing roughness. If roughness is too small, less than 0.1 μm, its effect on hysteresis can be neglected. In our case, roughness is in the range 0.01 μm, and thus it probably does not contribute to the observed hysteresis. Surface heterogeneity is a major cause of hysteresis in the case of segmented polymers such as poly(ether urethane urea)s[42]. On a pure PET film, the only surface heterogeneity is that of the repeat unit, which is in the scale range of a few angstroms. This scale is far too small to give rise to hysteresis[43]. Deformation of the surface area of a soft polymer can possibly alter the contact angle with a liquid[44,45] and this phenomenon might be different during immersion and emersion. Deformation may then be a cause of hysteresis. At room temperature, our PET sample is well below its glass transition temperature (which is around 70°C), so significant deformation is unlikely to occur.

Another possible cause of hysteresis is orientation and reorientation of macromolecules at the surface of the solid. In our case, the angle very quickly changes from its advancing to receding value: about 4 s in a high-speed (25 mm min^{-1}) experiment. This short time would imply rather fast rearrangements at the surface. Of course, the surface mobility might be higher than the bulk mobility, especially in the presence of water, which may act as a plasticizer. However, we do not believe in the possibility of such fast molecular rearrangements under our conditions. Our interpretation of the hysteresis observed in *Figure 1* is that it is due to the first step of swelling of the polymer surface layer by water, i.e. water adsorption. During immersion, water probes a mainly hydrophobic surface, and the contact angle is high (75–80°). In contact with the liquid, PET adsorbs water molecules: the receding contact angle then drops to 40°. In air, the weakly bonded water molecules desorb, restoring a hydrophobic surface: the contact angle (advancing) increases again to near 80°. By performing successive cycles, the total contact time of the PET sample with water progressively increases, which allows some water molecules to become more strongly bonded to PET: the second step of swelling starts. This more strongly bonded water does not have time to desorb during the stay of the sample in air of the immersion–emersion cycle. This accounts for the variation of the advancing contact angle from 80 to 75°, which can be seen on *Figure 1*. After contact with water, the surface structure is dominated by the weakly bonded adsorbed water, so the receding contact angle remains constant.

A prolonged contact time (several tens of hours) of the PET film in water gives rise to a marked decrease of both advancing and receding contact angles (*Figure 2*). It is then reasonable to consider that molecular rearrangements have time to take place. Extended swelling of the surface region could also occur and explain the angle's decrease. However, equilibrium swelling is reached long before 70 h whereas it takes 70 h for the angles to stabilize. This situation is similar to the one described by Lavielle and Schultz[5] in the case of acrylic acid-grafted polyethylene where water adsorption and/or absorption equilibrium is reached long before contact angle equilibrium. The hysteresis increases because θ_R decreases more rapidly than θ_A. Again, we interpret hysteresis by a fast adsorption–desorption phenomenon. The increase in $\Delta\theta$ seems to indicate that the amount of water adsorbed on a rearranged PET surface is higher but is not more strongly adsorbed because it desorbs in air as quickly as in the case of the non-rearranged surface. It can be seen in *Figure 2* that contact angles reach a plateau after a 70 h contact time in water. At this stage, we cannot say if this plateau represents a true thermodynamic equilibrium state. Shanahan *et al.*[16] have shown a contact angle hysteresis on PET but by the use of another technique and without giving the time course of their experiments, rendering a comparison with our data difficult.

Left in air for over 50 h, a sample previously 'equilibrated' with water does not recover its original hydrophobic state as indicated in *Figure 3*. This tends to become a classical result as mentioned in papers by Lavielle and Schultz[5] and Yasuda *et al.*[46]. Orientation in water is possibly made easier by a plasticizing effect of water and water might have a stronger 'orientating strength' than air[46].

Figure 4 shows a clear temperature effect on the dynamic contact angles. Several factors may contribute to the observed decrease of contact angles with increasing temperature. An increase in temperature gives rise to a decrease of all interfacial energies. So, if γ_{SA} (solid–air interfacial energy) and γ_{SW} (solid–water interfacial energy) decrease in such a way that the difference $\gamma_{SA}-\gamma_{SW}$ remains almost constant (or increases), a decrease in γ_{WA} (water surface energy) will automatically imply a decrease in the solid–water contact angle. The swelling of PET by water also increases with increasing temperature, so the contact angles will decrease due to this effect as well. And finally, an increase in chain mobility may favour molecular rearrangements and enhance surface polarity as discussed above. It is difficult to evaluate the relative importance of these factors. The fact that θ_R exhibits a more marked decrease near 70°C, which happens to be close to the glass transition temperature of PET, seems to indicate that surface conformational changes are likely to occur at least in the last part of the curve. In the case of long contact time with water, where we interpreted the angle's decreases in terms of molecular rearrangements, it was also θ_R that was more sensitive than θ_A.

Another way to study the phenomenon of equilibration of a polymeric surface with water is static tensiometry (*Figure 5*). The equilibrium contact angles are reached in 9 to 10 days. It is most likely that a true thermodynamic equilibrium is achieved. Vallat *et al.*[47] observed similar results on amorphous PET in contact with water for long times and probing the surface with an air bubble or an alkane droplet. A pseudo-plateau between 10^3 and 10^4 s was also observed by these authors. It is difficult to interpret these results precisely. Our experimental procedure is more convenient than theirs, as it merely requires recording the mass as a function of time. The initial receding angle is surprisingly high (53°, *Figure 5*). This might be due to a weight increase of the sample by water swelling. The value of 53° has thus to be considered cautiously and will not be used in the quantitative treatment of the static tensiometry data presented below.

Let us now comment on the results of the conformational calculations. *Figure 6* shows that the conformations with an energy less than $3\,\mathrm{kcal\,mol^{-1}}$ above the minimum represent 55% of the conformational space. The percentage reaches 80% when $5\,\mathrm{kcal\,mol^{-1}}$ is taken as the limit. This demonstrates the highly flexible character of the molecule along the $O–CH_2–CH_2–O$ sequence. The remaining 20% correspond to conformations inaccessible for steric reasons. The conformational map also reveals the existence of a centre of symmetry, the M1 state (*Figure 6*), described by the pair $(\phi, \psi) = (180, 180)$. The M1 and M5 states are 'stretched conformations', whereas the M2, M3 and M4 states are rather 'bent conformations'. If the M1 and M5 conformations are highly represented along the chain, the macromolecule will tend towards a planar zig-zag conformation like in a crystal[48]. On the other hand, if M2, M3 and M4 are dominant, the macromolecule will adopt a random-coil conformation like in a bad solvent. That is the reason why M1 and M5 are mentioned in *Table 1* as associated with an organized state and M2, M3 and M4 with a coil state.

Our calculations correlate with infra-red spectroscopy results. Koenig *et al.*[49] have shown that the *trans* conformation (corresponding to our M1 state) represented 13–18% of the total conformations in an amorphous PET film (our calculation gave 12.2%).

Tables 2 and *3* show that, if CH_2I_2 affects very little the distribution of conformations in PET, there is a dramatic effect of water. The organized/coil ratio $(M1+M5)/(M2+M3+M4)$, equal to 26/74 in the free state, remains very close in CH_2I_2 (30/70) but becomes 74/26 in water (*Table 3*). The molecule tends to stretch in water. PET–CH_2I_2 interactions are weak, so the macromolecule remains mainly in a coil conformation in order to favour the PET–PET interactions. However, with water, the possibility of hydrogen bonding exists between the ester groups and H_2O. The molecule then spreads out in order to expose its ester groups to water and maximize the possibility of hydrogen-bond formation. This process most probably takes place when PET is contacted with water for a sufficient time at a sufficient temperature.

When molecular rearrangements at the surface of a polymer are invoked in order to interpret contact angle hysteresis data, authors speak in terms of revealing or burying polar groups (and vice versa, burying or revealing apolar groups). This is easy to conceive, for instance, in the case of polar groups grafted onto an apolar chain. Molecular rearrangements at the surface of a polymer like PET, where relatively polar groups (esters) alternate with apolar ones at a scale of a few tens of angstroms, are much less clear to imagine. This work sheds light on the process.

It is interesting to go a step further and to compare quantitatively the molecular modelling part and the contact angle data. Theoretically, the energy change when the system goes from the free state (or the state where it is in contact with an aprotic poor solvent, which is also equivalent to a chain in contact with air) to the state where it is in contact with water can be calculated. The energy of a chain in a given state is the sum of the energies of the different conformers, each energy being multiplied by its statistical weight. The energy change can then be written as follows:

$$\Delta E_c = \sum_i p_i E_i(\text{final}) - \sum_i p_i' E_i'(\text{initial})$$

with p_i and E_i being the probability and energy of conformer i in the final state (chain in contact with water) and p_i' and E_i' being the probability and energy of conformer i in the initial state (free chain or chain in contact with air). This term ΔE_c can be compared with the solid–liquid interfacial energy drop $\Delta\gamma$ observed when the solid, equilibrated with air, is dipped into water and adjusts its surface conformations to reach equilibrium with water. The assumption is made that the interfacial energy drop is solely due to the conformational change. The PET film, equilibrated with air, is contacted with water at time zero. The initial contact angle is θ_{Ai}. Once equilibrium with water is reached, the advancing contact angle has dropped to θ_A. One can write:

$$\text{at time zero} \qquad \gamma_l \cos\theta_{Ai} = \gamma_{sv} - \gamma_{sli}$$

$$\text{at equilibrium} \qquad \gamma_l \cos\theta_A = \gamma_{sv} - \gamma_{sl}$$

with γ_l = liquid surface energy, γ_{sv} = solid–vapour interfacial energy, γ_{sli} = initial solid–liquid interfacial energy, γ_{sl} = final solid–liquid interfacial energy, θ_{Ai} = initial advancing angle of water on the PET film out of equilibrium and θ_A = advancing angle of water on the PET film equilibrated with water.

Then

$$\Delta\gamma = \gamma_{sli} - \gamma_{sl} = \gamma_l(\cos\theta_A - \cos\theta_{Ai})$$

$\Delta\gamma$ being equal to ΔE_c if a small entropic term is neglected (see below):

$$\Delta E_c = \gamma_l(\cos\theta_A - \cos\theta_{Ai})$$

This latter equation allows the comparison of the theoretical calculations with the contact angle data. Using data in *Tables 1* to *3*, ΔE_c can be calculated. It is found to be $8.6\,\mathrm{mJ\,m^{-2}}$. On the other hand, using static contact angle data of *Figure 5*, $\Delta\gamma$ is determined as being $13.4\,\mathrm{mJ\,m^{-2}}$. The agreement is rather good, taking into account all the assumptions that have been made. A similar treatment could apply to the receding angles but, since we are not sure of the value of the initial receding angle, the calculations are not presented.

The last point is to estimate the error made when neglecting the entropic contribution to the surface energy.

Generally speaking, it is far from being negligible, as shown by Haidara *et al.*^{50}, who developed a method, based on contact angle measurements as a function of temperature, to estimate the entropic contribution to surface energy. However, our problem is not the same, as we deal with surface-energy differences ($\Delta\gamma$) between surfaces equilibrated with air and water. Is there a significant difference between the entropy of a chain at the surface of a PET sample in contact with air or with water? In other words, is there a significant difference in the chain mobility at a surface in contact with air or water? Adsorption of water molecules on PET by hydrogen bonding could decrease the mobility. On the other hand, water could slightly plasticize the PET surface, increasing mobility. The balance is probably close to zero and thus the entropic contribution to the surface energy almost vanishes in the surface-energy difference $\Delta\gamma$.

CONCLUSION

Surface restructuring of polymers put in different media is currently widely accepted. However, in a polymer like PET, without side chains or block structure, the exact nature of the rearrangements initially appeared to be rather mysterious. Molecular modelling helped us to describe the restructuring process of the polymer when going from air to water. In air, 'bent' conformers are dominant, which implies a coil-like structure of the macromolecule. In this situation the PET–PET interactions are predominant. On the other hand, in water, 'stretched' conformers become the majority, and the chain adopts a conformation that tends towards the planar zig-zag structure of the molecules in crystals. This structure favours the PET (ester groups)–water interactions by hydrogen bonding. This part of our work constitutes an illustration of the high potential of molecular modelling in polymer science.

We tried to find a quantitative confirmation of the conformational calculations in the contact angle data. This was possible by considering the contact angle evolution together with the conformational restructuring at the surface of a sample, previously equilibrated with air and subsequently put in contact with water. The agreement between experimental and calculated data was reasonable.

The results presented in this paper concern an amorphous PET film. It would be interesting to investigate the effect of increasing crystallinity. Normally, crystallinity should hinder surface restructuration for two reasons: the decrease in molecular mobility and the fact that the structure in the crystal resembles the conformations of equilibrium with water. However, crystallinity at the surface may be different from crystallinity in the bulk and rather unexpected results might be obtained.

ACKNOWLEDGEMENTS

We thank the Rhône-Poulenc Company for financial support and permission for publication. We are indebted to Dr I. Tvaroska, Slovak Academy of Science, Bratislava, Czechoslovakia, for providing the 'Solvol' software.

REFERENCES

1 Lavielle, L. in 'Polymer Surface Dynamics' (Ed. J. D. Andrade), Plenum, New York, 1988, p. 45
2 Langmuir, I. *Science* 1938, **87**, 493
3 Holly, F. J. and Rejofo, M. F. *J. Biomed. Mater. Res.* 1975, **9**, 315
4 Ratner, B. D. and Yoon, S. C. in 'Polymer Surface Dynamics' (Ed. J. D. Andrade), Plenum, New York, 1988, p. 137
5 Lavielle, L. and Schultz, J. *J. Colloid Interface Sci.* 1985, **106**, 438
6 Yasuda, H., Sherry, B., El Nokaly, M. A. and Friberg, S. E. *J. Appl. Polym. Sci.* 1982, **27**, 1735
7 Ruckenstein, E. and Gourisankar, S. V. *J. Colloid Interface Sci.* 1986, **109**, 557
8 Kessaissia, Z., Papirer, E. and Donnet, J. B. *J. Colloid Interface Sci.* 1981, **79**, 257
9 Andrade, J. D., Gregonis, D. E. and Smith, L. M. in 'Surface and Interfacial Aspects of Biomedical Polymers', Vol. 1 (Ed. J. D. Andrade), Plenum, New York, 1985, Ch. 2, p. 15
10 Andrade, J. D. in 'Polymer Surface Dynamics' (Ed. J. D. Andrade), Plenum, New York, 1988, p. 1
11 Andrade, J. D., Gregonis, D. E. and Smith, L. M. in 'Physicochemical Aspects of Polymers Surfaces', Vol. 2 (Ed. K. L. Mittal), Plenum, New York, 1983, p. 911
12 Andrade, J. D. and Chen, W. Y. *Surf. Interface Anal.* 1986, **8**, 253
13 Brouwer, W. M. *Colloids Surf.* 1989, **40**, 235
14 Okubo, M., Yamamoto, Y. and Kamei, S. *Colloid Polym. Sci.* 1989, **267**, 861
15 Lavielle, L., Schultz, J. and Sanfeld, A. *J. Colloid Interface Sci.* 1985, **106**, 446
16 Shanahan, M. E. R., Carre, A., Moll, S. and Schultz, J. *J. Chim. Phys.* 1986, **83**, 351
17 Shanahan, M. E. R., Carre, A., Moll, S. and Schultz, J. *J. Chim. Phys.* 1987, **84**, 199
18 Pennings, J. F. M. and Bosman, B. *Colloid Polym. Sci.* 1979, **257**, 720
19 Allinger, N. L. *J. Am. Chem. Soc.* 1977, **99**, 8127
20 Burckert, U. and Allinger, N. L. in 'Molecular Mechanics' (ACS Monograph 177), American Chemical Society, Washington, DC, 1982
21 Sundararajan, P. R. and Flory, P. J. *J. Am. Chem. Soc.* 1974, **96**, 5025
22 Suter, U. W. and Flory, P. J. *Macromolecules* 1975, **8**, 765; Yoon, D. Y., Sundararajan, P. R. and Flory, P. J. *Macromolecules* 1975, **8**, 776
23 Volkenstein, M. V. in 'Configurational Statistics of Polymeric Chains', Interscience, New York, 1959
24 Flory, P. J. in 'Statistical Mechanics of Chain Molecules', Interscience, New York, 1969
25 Flory, P. J. *Macromolecules* 1974, **7**, 381
26 Pierotti, R. A. *Chem. Rev.* 1976, **76**, 717
27 Tvaroska, I. and Kozar, T. *J. Am. Chem. Soc.* 1980, **102**, 6929
28 Andrade, J. D., Smith, L. M. and Gregonis, D. E. in 'Surface and Interfacial Aspects of Biomedical Polymers', Vol. 1 (Ed. J. D. Andrade), Plenum, New York, 1985, Ch. 7, p. 249
29 Wilhelmy, L. *Ann. Physik* 1863, **119**, 117
30 Padday, J. F. *Surf. Colloid Sci.* 1969, **1**, 39
31 Johnson, R. E. and Dettre, R. *Surf. Colloid Sci.* 1969, **2**, 85
32 Perez, S. and Brisse, F. *Acta Crystallogr. (B)* 1976, **32**, 470
33 Perez, S. and Brisse, F. *Can. J. Chem.* 1975, **53**, 3551; Perez, S. and Brisse, F. *Acta Crystallogr. (B)* 1977, **33**, 1673
34 Scott, R. A. and Scheraga, H. A. *J. Chem. Phys.* 1966, **44**, 3054; **45**, 2091
35 Brant, D. A., Miller, W. G. and Flory, P. J. *J. Mol. Biol.* 1967, **23**, 47
36 Smyth, C. P. in 'Dielectric Behaviour and Structure', McGraw-Hill, New York, 1955, p. 244
37 Ramachandran, G. N. *Int. J. Protein Res.* 1965, **1**, 5
38 Hopfinger, A. J. in 'Conformational Properties of Macromolecules', Academic Press, New York, 1973, p. 121
39 'Handbook of Chemistry and Physics', 55th Edn., CRC Press, Cleveland, OH, 1974; Riddick, J. A. and Bunker, W. B. in 'Organic Solvents', 3rd Edn., Wiley Interscience, New York, 1970
40 Smith, L., Doyle, C., Gregonis, D. E. and Andrade, J. D. *J. Appl. Polym. Sci.* 1982, **27**, 1277
41 Johnson, R. E. and Dettre, R. H. in 'Contact Angle, Wettability and Adhesion' (Ed. F. M. Fowkes), *Adv. Chem. Ser.* 1964, **43**, 112
42 Takahara, A., Jo, N. J. and Kajiyama, T. *J. Biomater. Sci. Polym. Edn.* 1989, **1**, 17
43 Neumann, A. W. and Good, R. J. *J. Colloid Interface Sci.* 1972, **38**, 341

44 Hansen, R. J. and Toong, T. Y. *J. Colloid Interface Sci.* 1971, **37**, 196

45 Jhon, M. S. and Yuk, S. H. in 'Polymer Surface Dynamics' (Ed. J. D. Andrade), Plenum, New York, 1988, p. 25

46 Yasuda, H., Sharma, A. K. and Yasuda, T. *J. Polym. Sci., Polym. Phys. Edn.* 1981, **19**, 1285

47 Vallat, M. F. Personal communication (to be published)

48 de Daubeny, R., Brown, C. J. and Bunn, C. W. *Proc. R. Soc. Lond. (A)* 1954, **226**, 531

49 Lin, S. B. and Koenig, J. L. *J. Polym. Sci., Polym. Phys. Edn.* 1982, **20**, 2277; Fina, L. J. and Koenig, J. L. *J. Polym. Sci., Polym. Phys. Edn.* 1986, **24**, 2525

50 Haidara, H., Pinhas, M. F. and Schultz, J. *C. R. Acad. Sci. Paris* 1992, **315** (II), 521; *J. Colloid Interface Sci.* submitted